Composite-hydroxide-mediated approach as a general methodology for synthesizing nanostructures†

Chenguo Hu,[*a] **Yi Xi,**[a] **Hong Liu**[*b] **and Zhong Lin Wang**[*c]

The composite-hydroxide-mediated (CHM) method is based on the use of molten composite hydroxides as a solvent in chemical reactions at $\sim$200 °C for the synthesis of a wide range of nanostructures. This review focuses on its recent development with an emphasis on its applications for synthesizing materials of complex oxides, hydroxides, simple oxides, sulfides, selenides, tellurides, fluorides and metals. The principle of this synthesis method is introduced, and the key factors that affect the morphology and size are studied. The advantages of its low synthesis temperature, low pressure and low cost are illustrated through the synthesis of functional wires, rods, belts and other nanostructures.

1 Introduction

Nanomaterials are intrinsically important because their properties differ significantly from those of their bulk counterparts. Nanomaterials are widely used in various applications such as energy cells,[1–5] sensitive sensors,[6–10] nanoelectronic devices[11–18] and bio-markers[19,20] etc. Consequently, the synthesis and fabrication of functional nanomaterials with predictable, rational strategies is a key for the development of their applications.

It is apparent that the full potential of the as-prepared nanostructures will only be realized when materials are not only synthesized in large quantities with reproducible size, shape, structure, crystallinity, and composition but also prepared and assembled using green, environmentally friendly methodologies.[21–24] There has been increasing interest in the development of clean synthetic procedures (green chemistry) for products targeted at biomedical applications, surface modifications and intrinsic property investigations. An environmentally acceptable solvent system and eco-friendly reducing and capping reagents are three essential elements for a completely green synthesis.

Nanocrystals have been prepared by many methods, including vapor phase process,[25,26] jet deposition,[26–28] milling,[29,30] sol-gel method,[31,32] microemulsion,[33] coprecipitation,[34] template syntheses,[35] hydrothermal synthesis[36–38] and solvothermal synthesis,[39,40] etc. Although all these methods have their own advantages, most of them involve high vacuum and a high temperature, or high pressure, or a low temperature with high pressures. The categories and mass of materials prepared by the vapor phase process and jet deposition syntheses are limited, which cause the high price of the products. Although milling processes can produce large quantities of crystal powders, the diameters of the produced particles are only sub-micrometer, and the morphology of the particles is difficult to control. The sol-gel and microemulsion methods are very practical syntheses and low cost methods for nanostructures, but they involve a final

aDepartment of Applied Physics, Chongqing University, Chongqing, 400044, P. R. China. E-mail: hucg@cqu.edu.cn
bState Key Laboratory of Crystal Materials, Shandong University, Jinan, 250100, P. R. China. E-mail: hongliu@sdu.edu.cn.
*cSchool of Materials Science and Engineering, Georgia Institute of Technology, Atlanta, Georgia, 30332-0245, USA. E-mail: zhong.wang@mse.gatech.edu*
† This paper is part of a *Journal of Materials Chemistry* theme issue on Nanotubes and Nanowires. Guest editor: Z. L. Wang.

Dr Chenguo Hu is a professor of Physics at Chongqing University. She received her Ph.D. from the Chongqing University. She presently is the Director of the Key Laboratory of Materials Physics of Chongqing City. Her research interests relate to the methodology of synthesis, and the properties and functions of nanomaterials.
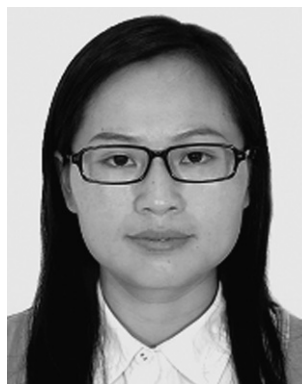
Chenguo Hu

Yi Xi obtained her M.Sc. in 2007 from Chongqing University, China. Currently she is pursuing her Ph.D. degree under the supervision of Prof. Chenguo Hu in Chongqing University, China. Her research interest in Ph.D. study is mainly focused on the preparation and correlative properties of sulfide and metal nanomaterials.

Yi Xi

calcination or annealing step at high temperature; thus they cannot be considered to be true low-temperature synthesis methods, and it is difficult to control the particle size and morphology. Hydrothermal and solvothermal syntheses are effective for synthesizing nanomaterials and available for many kinds of materials. However, some surfactants and capping agents used in hydrothermal or solvothermal methods are not completely removed from the final products, which can affect some of the physical properties of the crystals. In addition, large amounts of organic solvent used in solvothermal synthesis would bring about environmental pollution. Moreover, because of the high pressure involved in hydrothermal and solvothermal syntheses, sophisticated equipment is required. Various synthesis methods are reported to be capable of producing various nanostructures, but most of the methods are limited to synthesizing one type of or a specific collection of nanostructures,[25–40] except a general approach is available for utilizing the hydrothermal route to synthesise a large variety of nanoparticles using fatty acids as structure-directing agents.[41]

In this review, we introduce the composite-hydroxide-mediated (CHM) approach as a technically sound, environmentally friendly methodology for creating a wide range of important nanostructures. Specifically, we emphasize the categories of crystals synthesized by the CHM approach, covering complex oxides, hydroxides, simple oxides, sulfides, selenides, tellurides, fluorides and metals. We show the advantages of the CHM method for synthesis of functional wires, rods, belts and other nanostructures, as well as the investigations of properties and applications of these materials. The mechanism of the crystal growth is discussed, and the key factors affecting morphology and size are concluded from the analysis of the fabrication processes.

2 The CHM approach

While bulk oxides have long been prepared in hydroxide melts at temperatures from 350 °C to over 1000 °C,[42–46] the preparation of uniform nanostructures using the CHM method at lower

temperature has only arisen in consideration of the eutectic point of composite hydroxides by us in 2006.[47,48]

The CHM method is based on chemical reactions of materials in eutectic hydroxide melts at a temperature of $\sim$200 °C and ambient pressure in the absence of organic dispersants or capping reagents. Although the melting points of pure sodium hydroxide, potassium hydroxide and lithium hydroxide are above 300 °C (T_m = 323 °C for NaOH, T_m = 404 °C for KOH, and T_m = 477 °C for LiOH) the eutectic points for particular mixtures of these elements, NaOH/KOH = 51.5:48.5, LiOH/KOH = 0.31:0.69, and NaOH/LiOH = 0.71:0.29 are only about 165 °C, 225 °C and 220 °C, respectively. The mixed hydroxides play the role of the reaction medium. Normally, the synthesis process of the CHM method is a one-step process. All of the raw materials with a certain amount of mixed hydroxides are placed within the Teflon vessel at one time. Then, the nanostructures form within the vessel after heating in a furnace at a temperature of *ca.* 200 °C for several hours or days. The as-produced materials are crystalline with clean surfaces, which are favorable for further investigating their intrinsic properties[49–54] and surface functionalization. The CHM method is one of the simplest, most versatile, and cost-effective approaches available for obtaining crystalline, chemically purified, single phase powders at lower temperatures and often in overall shorter reaction times with few residual impurities, as compared with conventional high temperature solid-state reactions. The environmental appeal of this method arises from its intrinsic scalability, generality, and facility as well as its fundamental basis on the use of hydroxides as the reaction medium.

3 Synthesis of nanocrystals

Complex oxides

Complex oxides such as perovskite, spinel, and garnet possess many important properties including ferroelectricity, ferromagnetism, colossal magnetoresistance, semiconductivity, luminance, and optoelectricity. Synthesis and device fabrication using these functional oxides have attracted a lot of attention because

Hong Liu

Dr Hong Liu received his B.Sc degree from Shandong Institute of Light Industry in 1985, and his Ph.D. degree from Shandong University in 2001. He is a professor in State Key Laboratory of Crystal Materials, Shandong University, China. His research interests are related to synthesis of nanomaterials, the application of nanomaterials in gas and biosensors, environmental protection, and new energy sources.

Zhong Lin Wang

Dr Zhong Lin (ZL) Wang is a Regents' Professor, COE Distinguished Professor and Director, Center for Nanostructure Characterization and Fabrication, at Georgia Tech. He has authored and coauthored four scientific reference and textbooks and over 520 peer reviewed journal articles, 55 review papers and book chapters, edited and coedited 14 volumes of books on nanotechnology, and holds 20 patents and provisional patents. He is in the world's top 25 most cited authors in nanotechnology from 1992 to 2002. His entire publications have been cited over 22000 times. The H-index of his citations is 72.

This journal is © The Royal Society of Chemistry 2009

J. Mater. Chem., 2009, **19**, 858–868 | 859

the physical properties can be tuned through full/partial element substitution. We have first demonstrated the feasibility of the CHM approach for the synthesis of single-crystalline complex oxide nanostructures of various structural and compositional motifs.[47] Up to now, twelve complex oxides has been synthesized by the CHM approach, including $BaTiO_3$, $BaMnO_3$, Fe_3O_4, $CoFe_2O_4$, $Pb_2V_2O_7$, $SrTiO_3$, $CuAlO_2$, $BaNbO_3$. etc.[47,48,53,54] $LiCoO_2$ nanocrystals have also been synthesized using mixed CsOH and KOH as a reaction medium by another group.[55]

In principle, complex oxide nanostructures of perovskite (ABO_3), spinel (AB_2O_4), delafossite (ABO_2), fluorite, etc., can be obtained *via* the CHM method, based on a reaction between a metallic salt (for A cation) and a metallic oxide (for B cation and O anion) with valence states that match those present in the desired product. For example, $Pb_2V_2O_7$ and $BaMnO_3$ nanobelts have been prepared with $Pb(NO_3)_2$ and V_2O_5, $BaCl_2$ and MnO_2, respectively (Fig. 1a,b). With full/partial substitution of the A site or B site ion, different complex oxides can be obtained. $BaMn_{1-x}Ti_xO_3$ nanorods (Fig. 1c) were obtained by partially replacing MnO_2 with TiO_2 in the preparation of $BaMnO_3$, whereas $Ba_{1-x}Sr_xTiO_3$ (Fig. 1d) was obtained by fully replacing MnO_2 with TiO_2 and partially replacing $BaCl_2$ with $SrCl_2$ in the preparation of $BaMnO_3$.[47]

The following reactions summarize a postulated mechanism for the synthesis of the $BaMnO_3$ nanorods. Here, the term M represents either Na or K:

$$2MOH + MnO_2 \rightarrow M_2MnO_3 + H_2O \qquad (1)$$

$$BaCl_2 + 2MOH \rightarrow Ba(OH)_2 + 2NaCl \qquad (2)$$

$$M_2MnO_3 + Ba(OH)_2 \rightarrow BaMnO_3\downarrow + 2MOH \qquad (3)$$

According to the classical crystal growth theory,[56,57] we believe a crystal growth experiences a dissolution–nucleation–aggregation–recrystallization process in the composite hydroxide melts. The dissolubility of reactants in the melts is based on the acid–base chemistry described by classical Brønsted theory.[58,59] The hydroxide ions of the melts dissociate into H_2O and O^{2-} ions, in much the same way that water in aqueous solutions dissociates into H_3O^+ and OH^- ions:

$$2OH^- \leftrightarrow H_2O \text{ (solution)} + O^{2-} \text{ (solution)} \qquad (4)$$
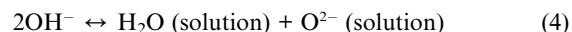
Thus, melts rich in H_2O are acidic and melts rich in O^{2-} are basic. In general, metal oxides are soluble in acidic and/or basic melts, not in neutral melts. The dissolution of reactants in the melts can be controlled by varying the H_2O and/or O^{2-} content.

Since the obtained sodium and potassium hydroxides contain 0.6% and 14.8% H_2O, respectively,[60] the water content is ~8.7% in the melts at a Na/K mole ratio of 51 to 49. Because the water content and the atmosphere over the melts in the covered Teflon vessel are fixed at a certain temperature in the process of the CHM synthesis, we propose that the initial water content in the melts should be an important factor affecting the dissolution of reactants. To demonstrate the influence of dissolubility, we varied the acidity (pH2O value) by adding a small amount of water in the melts in the preparation of $BaMnO_3$. Obviously, we can see the length of the $BaMnO_3$ nanorods is shortened with additional water (Fig. 1e,f) due to the fact that the faster dissolution of MnO_2 results in the acceleration of crystallization and precipitation of $BaMnO_3$ nanocrystals. Consequently, a higher acidity is beneficial for an isotropic growth of crystals.[48] Accordingly, we can conclude that the acidity of the melts is a key factor for the control of growth of crystals in the hydroxide melts.[61]

The *I–V* curves of the film made from the $BaMnO_3$ nanorods exhibit different weak rectifying characteristics at low and room temperature (Fig. 2a,b) because of the formation of the contact barriers caused by surface band bending and Fermi level pinning
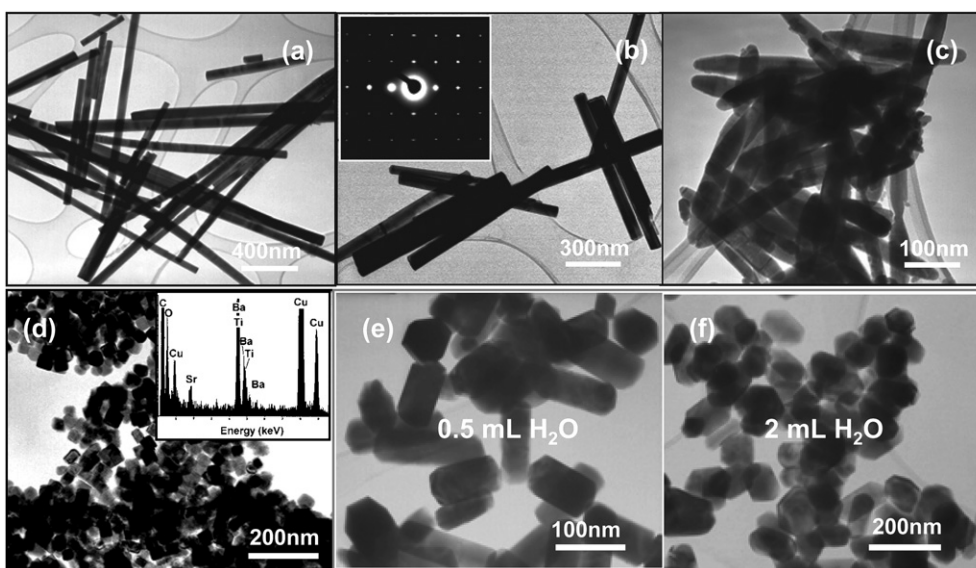
Fig. 1 TEM images of (a) $Pb_2V_2O_7$ nanobelts prepared at 200 °C for 24 h, (b) $BaMnO_3$ nanorods obtained at 170 °C for 72 h, (c) $BaMn_{0.5}Ti_{0.5}O_3$ nanorods obtained at 200 °C for 48 h, (d) $Ba_{1-x}Sr_xTiO_3$ nanocubes obtained at 200 °C for 24 h, and $BaMnO_3$ nanorods obtained at 200 °C for 120 h with added (e) 0.5 mL and (f) 2 mL H_2O.[48]
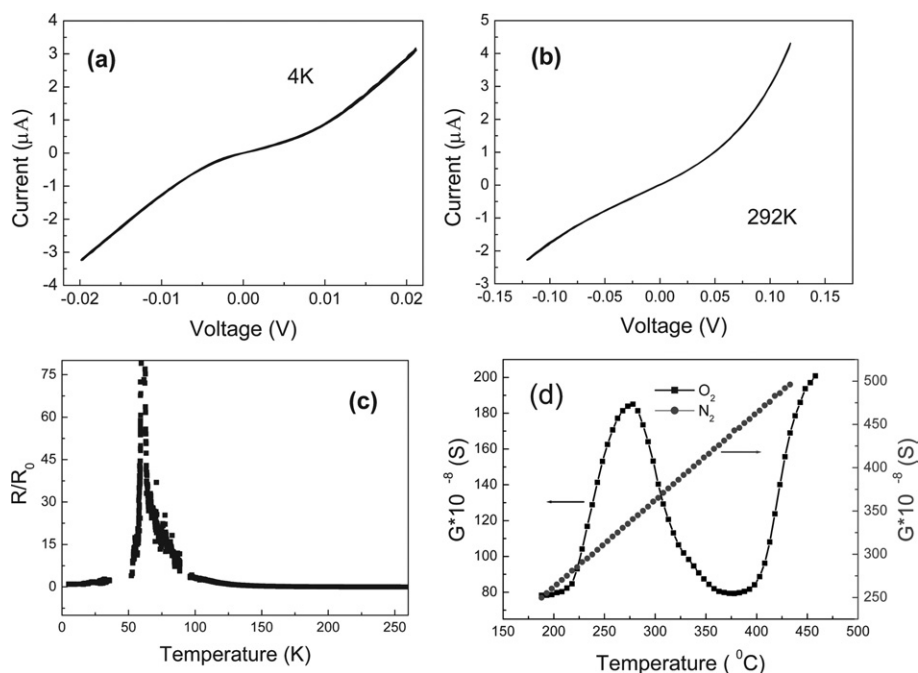
Fig. 2 *I–V* curves at (a) 4 K and (b) room temperature, and relative resistance vs. temperature plot (c) and conductivity vs. temperature curves under N_2 and H_2 atmospheres for the sample of $BaMnO_3$ nanorods grown at 200 °C for 120 h.[48,51]

of the nanorods.[62] The degradation of the rectifying characteristic is attributed to the decrease of contact barrier on account of the increase of metal resistance at room temperature. A relative resistance vs. temperature plot from 4 to 250 K for the film of the $BaMnO_3$ nanorods is given in Fig. 2c. The large peak can be seen at 58 K from the plot, which indicates the phase transition occurs at this temperature,[48] which also agrees with other group's result.[63] The gas sensitivity of the sensor based on the $BaMnO_3$ nanorods reveals that it has a sensitive response to oxygen gas but no response to nitrogen gas. We can see a monotonous conductivity in N_2 atmosphere, which exhibits a normal semiconductor characteristic of $BaMnO_3$ nanorods and a strong conductivity peak in oxygen atmosphere caused by chemical adsorption of oxygen ions (Fig. 2d). Since the intrinsic electric conductance increases linearly with the temperature, but the oxidation chemical adsorption makes the electric conductance decrease, the competition of these two factors under different temperatures results in the presence of the electrical conductance peak.[51]

Hydroxides

Hydroxides have many potential applications.[49,64] The surface hydroxyl groups may act as active sites for possible surface modification through condensation reactions with amino acids or biologically active molecules. Thus, hydroxide nanocrystals may have potential in the field of biological labeling and antibacterial applications. In addition, the similarity of the crystal structure and lattice constants suggests that doped hydroxide nanocrystals could be prepared by a similar growth process, as lattice mismatching would not be a serious concern. Meanwhile, because hydroxides can be easily converted into oxides or sulfides through dehydration or sulfuration, a hydroxide or co-doped

hydroxide nanocrystal can act as an important precursor for preparing the corresponding oxide or sulfide nanocrystal.

The CHM approach gives a facile method of synthesizing hydroxides. To obtain hydroxides, the only material needed is metallic salt. The metallic salt would reacts with NaOH/KOH/LiOH at a temperature of 165–220 °C in the course of 1–48 h to produce an insoluble hydroxide. Some hydroxides have been synthesized by the CHM approach in our laboratories, such as $La(OH)_3$ nanobelts (Fig. 3), $Cd(OH)_2$ and $Dy(OH)_3$ nanoflakes, and $Mg(OH)_2$ nanolamellae. The length of these single crystalline nanobelts of $La(OH)_3$ can be easily manipulated *via* changing the growth time (Fig. 3a,c), because the prolongation of time would allow a bigger crystal to grow and a smaller crystal (less than critical size) to dissolve.[65] Thus, we note another factor, the growth time, that affects the crystal morphology in the CHM method.

The simple chemical reaction to form $La(OH)_3$ (where M denotes Na or K) is as follows:

$$La(CH_3COO)_3 + 3MOH \rightarrow La(OH)_3\downarrow + 3M(CH_3COO) \quad (5)$$
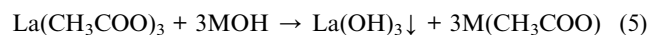
Both the fluorescence and conductivity of the $La(OH)_3$ nanobelts (Fig. 4) reveal the nanobelts have potential applications in biological labeling and sensing.

Simple oxides

Simple oxides possess unique properties and functions which can be further developed *via* doping and partial substitution with other elements. The synthesis of simple oxides is a fundamental technique to explore the preparation of complex oxides. In principle, the synthesis of simple oxides follows the same route as for the synthesis of hydroxides through the CHM approach.
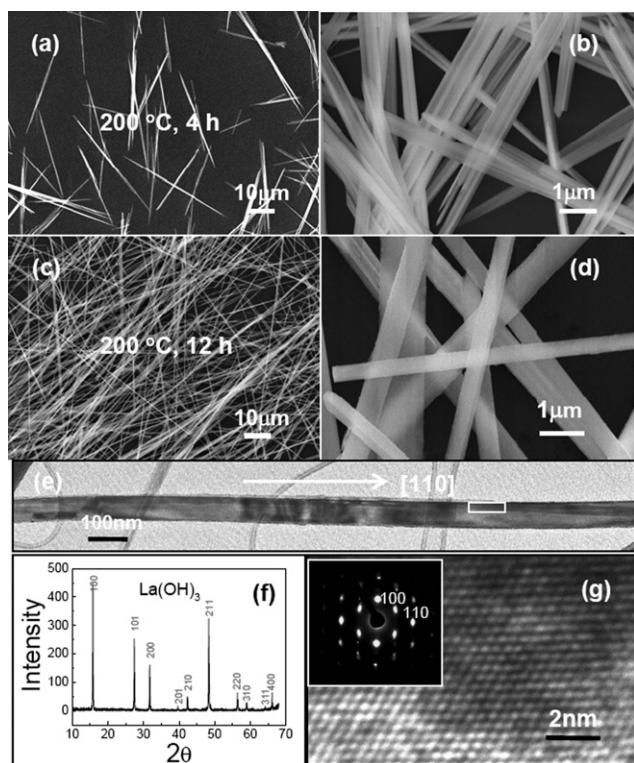
Fig. 3 SEM images of La(OH)$_3$ synthesized at 200 °C for 4 h (a,b) and 12 h (c,d). TEM image of a single La(OH)$_3$ nanowire (e). XRD spectrum (f) and HRTEM image (g) with electron diffraction pattern (inset).[49]
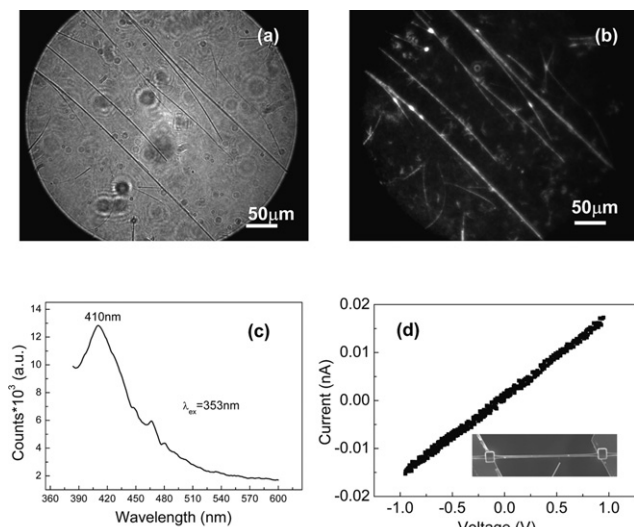
Fig. 4 Bright-field (a) and fluorescence (b) images of a bundle of La(OH)$_3$ nanobelts under UV excitation. PL emission spectrum (c) of La(OH)$_3$ at an excitation wavelength of 353 nm. Current–voltage (I–V) plot (d) of a single nanobelt, showing the constant resistivity and SEM image of the single nanobelt electrode (inset).[49]

Nanocrystals are obtained from the reaction between a dissoluble metal salt and the medium at temperature of 200 °C for a few hours or days. We have synthesized Cu$_2$O,[66] Bi$_2$O$_3$, BaO, ZnO, CeO$_2$,[67] CuO, Fe$_2$O$_3$, and NiO micro- to nanocrystals using the CHM method. Fig. 5a–c show the SEM images of Cu$_2$O

nanowires prepared from CuCl, Bi$_2$O$_3$ microrods obtained fromBi(NO$_3$)$_3$·5H$_2$O, and BaO nanowires synthesized from BaCO$_3$. The reaction to form simple oxides in the hydroxide melts, such as Cu$_2$O, is as follows (where M denotes Na or K):

$$CuCl + MOH \rightarrow CuOH + MCl \qquad (6)$$

As is well known, CuOH is not stable, especially at high temperature, and it then forms Cu$_2$O and water.

$$2CuOH \rightarrow Cu_2O\downarrow + H_2O \qquad (7)$$

The morphology of the crystals changes from small spheres assembled by nanoflakes to Cu$_2$O nanostars and nanowires with rising temperature from 170 °C to 220 °C for the same growth time (Fig. 5d–f).[66] Therefore, we come to the conclusion that the morphology can be tuned by the growth temperature.

As viscosity is rather high in the hydroxide melts at temperatures less than 200 °C, it greatly reduces the speed of nucleus aggregation and recrystallization. Consequently, the slow diffusion speed of matter in the melts prevents crystal from growing large. Previously, Dauby and co-workers have investigated the conductivity in the eutectic hydroxide melts and obtained the result that the conductivity increases with rising temperature.[68] According to this result, we believe the viscosity of the hydroxide melts decreases with rising temperature. From the evolution of the Cu$_2$O crystal morphology at varied temperatures, we can conclude that lower viscosity tends to yield larger crystals. Actually, it is a principle that bulk crystals have grown in hydroxide fluxes at high temperature.[42–46] Hence, a suitable viscosity of the melts can help obtain well-defined morphology as desired.

Doping an oxide can not only transform its morphology, but also change its physical properties, as illustrated through the example of Ba-doped CeO$_2$.[52] Ba-doped CeO$_2$ nanowires have been obtained from doping CeO$_2$ particles through the CHM approach, as is shown in Fig. 6a–d. Test results for humidity sensitivity based on CeO$_2$ particles, and Ba-doped CeO$_2$ nanowires of short and long length, indicate that both doping Ba into CeO$_2$ and converting the morphology into a nanowire can improve the humidity sensitivity (Fig. 6e,f).

Chalcogenides

Many metal elements can combine with chalcogen to form stable crystalline semiconductor phases that exhibit a variety of unique optical and electrical properties.[69] From an overview of the conventional solid state chemical synthesis in hydroxide melts, researchers have never tried this method for synthesizing other crystals than oxide bulk crystals. Our target is to develop the CHM approach as a general methodology in the synthesis of various kinds of functional nanocrystals.

In a typical synthesis of chalcogenides, the metal element is provided from metallic salts (such as nitrates, chlorates, carbonates and acetates, etc.) and chalcogen element is provided from chalcogen powder (such as sulfur powder or Na$_2$S, selenium powder and tellurium powder).[70,71] The synthesis of metal sulfides needs no reducing reagents, but metal selenide and telluride need reducing reagents, such as hydrazine and ethylenediamine. For
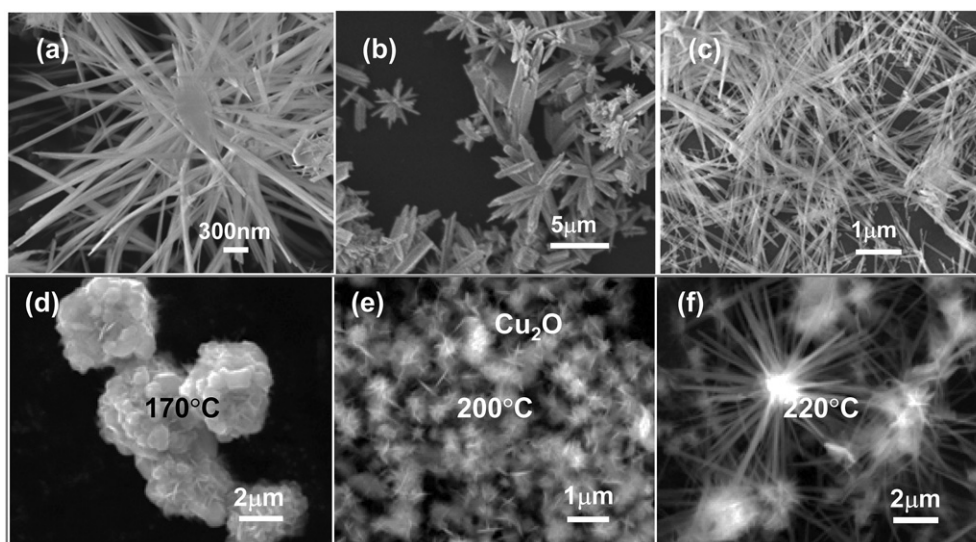
Fig. 5 SEM images of Cu$_2$O nanowires (a) synthesized at 200 °C for 24 h, Bi$_2$O$_3$ nanorods (b) synthesized at 200 °C for 6 h and BaO nanowires (c) synthesized at 200 °C for 6 h. SEM images of Cu$_2$O crystals prepared at 170 °C (d), 200 °C (e) and 220 °C (f) for 24 h.[66]
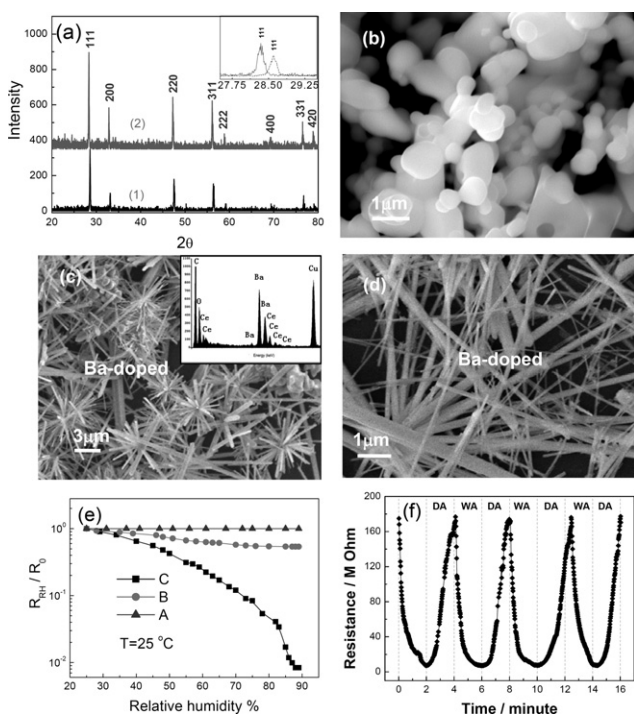

Fig. 6 XRD spectra of the source material CeO$_2$ (1) and Ba-doped CeO$_2$ nanowires (2) synthesized at 200 °C for 72 h (a), SEM images of CeO$_2$ (b) and the Ba-doped CeO$_2$ sample prepared at 200 °C for 48 h (c) and 72 h (d). Static response of the devices made of source material CeO$_2$ (A), and Ba-doped CeO$_2$ nanowires grown for 12 h (B) and 72 h (C) to humidity (e). Dynamic response of the Ba-doped CeO$_2$ grown for 72 h to humidity (f). Here DA denotes dry air and WA denotes wet air.[52]

example, CdS wires have been produced from the reaction between 0.5 mmol CdCl$_2$·2.5H$_2$O and 0.5 mmol Na$_2$S·9H$_2$O at 200 °C for 6 h (Fig. 7a), and Cu$_2$S nanobelts have formed from the reaction between 1 mmol CuCl and 0.5 mmol Na$_2$S·9H$_2$O at 165 °C for 8 h (Fig. 7b) by the CHM method. The ZnSe nanorods

have been prepared from Zn(NO$_3$)$_2$·6H$_2$O and Se powder at 0.5 mmol each with 2 mL N$_2$H$_4$·H$_2$O at 200 °C for 24 h (Fig. 7c), and Cu$_2$Se nanoflakes have been prepared from 1 mmol CuCl$_2$·2H$_2$O, 0.5 mmol Se powder and 2 mL N$_2$H$_4$·H$_2$O at 200 °C for 24 h (Fig. 7d). The Ag$_2$Te nanowires have been synthesized from 1 mmol AgNO$_3$, 0.5 mmol Te powder, 1.5 mL H$_2$NCH$_2$CH$_2$NH$_2$ and 1.5 mL N$_2$H$_4$·H$_2$O at 180 °C for 36 h (Fig. 7e), and PbTe nanorods have been synthesized from Pb(NO$_3$)$_2$ and Te powder at 0.5 mmol each with 3 mL N$_2$H$_4$·H$_2$O at 200 °C for 48 h (Fig. 7f).[50] Other chalcogenides have also been obtained including ZnS, PbS, Bi$_2$S$_3$, Zn$_{0.5}$Cd$_{0.5}$S, CdSe$_x$S$_{1-x}$, CdSe, PbSe, Zn$_x$Cd$_{1-x}$Se, CdTe micro- and nano-structures by the CHM approach.[70,71]

In the hydroxide melts, an obvious understanding of the reaction is the disproportionation reaction of the chalcogen occurring in the alkaline conditions.[72] That is:

$$3E + 6OH^- \rightarrow 2E^{2-} + EO_3^{2-} + H_2O \text{ (E denotes S, Se or Te)} \quad (8)$$
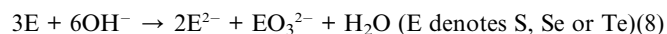
Whereas, owing to the increasing metallic property of S, Se and Te, different chalcogens have different reactive processes. Based on the electrode potential analysis, the occurrence probability of the disproportionation reaction to S, Se, Te is in a sequence of S > Se > Te. Our experiments demonstrate this fact that metal sulfide crystals can be synthesized successfully by the CHM approach without any reducing reagent, but selenides and tellurides can not, and the growth time is in a sequence of sulfides < selenides < tellurides. In addition, the size of the produced sulfides is usually larger than that of selenide and tellurides.

In the hydroxide melts, the form of CdS crystal follows a dismutation reaction (where M denotes Na or K),

$$6MOH + 3S \rightarrow 2M_2S + M_2SO_3 + 3H_2O \quad (9)$$

$$M_2S + CdCl_2 \rightarrow 2M_2Cl + CdS\downarrow \quad (10)$$
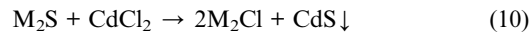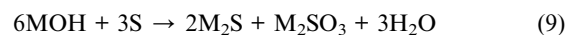
But the formation of selenides and tellurides is more complex. The growth mechanism of PbTe nanorods has been carefully

This journal is © The Royal Society of Chemistry 2009

J. Mater. Chem., 2009, **19**, 858–868 | 863
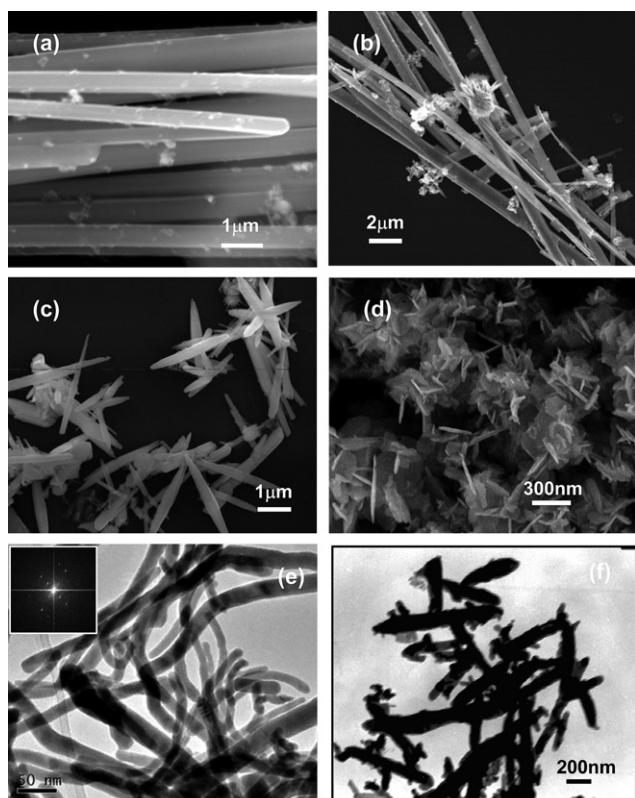
Fig. 7 SEM images of (a) CdS microwires synthesized at 200 °C for 6 hours, (b) Cu$_2$S nanobelts synthesized at 165 °C for 8 h, (c) ZnSe nanorods prepared at 200 °C for 24 h, (d) Cu$_2$Se nanoflakes prepared at 200 °C for 24 h. TEM images of (e) Ag$_2$Te nanowires synthesized at 180 °C for 36 h and (f) PbTe nanorods synthesized at 200 °C for 48 h. FFT of a single Ag$_2$Te nanowire (inset in (e)).[66,67,50,73]
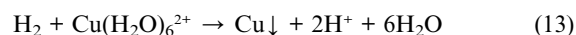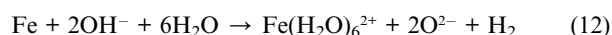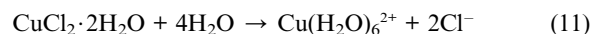
investigated *via* UV-vis spectra in different solutions related to the reaction steps, indicating that the polymerized tellurium anions and metal(II) amides (Pb(N$_2$H$_4$)$_2$) in the hydrazine hydroxide melts control the growth process of the PbTe nanostructures.[43] The Te rings and Pb(NH$_2$)$_2$ reduce the free ions concentration in the solution through slowly releasing the Te^{2-} or Pb^{2+} ions, and reduce the speed of reaction, which is favorable for separating the growth step from the nucleation step and crystallization. So the PbTe nuclei preferentially grow along a certain direction to form the nanorod. The whole process can be described diagrammatically as shown in Scheme 1.

The phase-transition-dependent conductivity and thermoelectric properties of silver telluride nanowires (Fig. 7e) have been investigated,[50] as shown in Fig. 8. The reversible structural phase transitions of the Ag$_2$Te nanowires from monoclinic structure (β-Ag$_2$Te) to face-centered cubic structure (α-Ag$_2$Te) around 148 and 133 °C are observed during the heating and

cooling process, respectively (Fig. 8A). The phase transition latent heat of the nanowires is much smaller compared to those of the thin film and the bulk of Ag$_2$Te, indicating that atom rearrangement from the monoclinic structure to the face-centered cubic structure is easier in one dimension than that in three or two dimensions. The abrupt changes in the temperature dependence of the electrical conductivity and the Seebeck coefficient are attributed to the structural phase transition (Fig. 8B). The thermal emf increases monotonically with the increase in temperature during both cooling and heating (Fig. 8C). The maximum Seebeck coefficient is ~170 and ~160 μVK^{-1} during the heating and cooling process, respectively (Fig. 8D), indicating a promising one-dimensional thermoelectric material as a building block for the construction of nanodevices.

Metals

Metal nanostructures have been of extensive interest in many different areas because of their unique or improved electronic, catalytic, optical, magnetic and other related properties. Micro- and nano-structures of elemental metals can be obtained by starting from reactants of metallic salts and metal Zn or Fe powder by the CHM approach at a temperature of 165–220 °C.[74] For example, Cu nanowires have been synthesized from 0.5 mmol CuCl$_2$·2H$_2$O and Fe powder at 200 °C for 16 h (Fig. 9a,c), and Sn cubes have been synthesized from 0.5 mmol SnCl$_2$·2H$_2$O and Zn powder at 200 °C for 6 h (Fig. 9b,c). Other metals obtained by the CHM approach include Ag, Pd, Sn, Bi and Ni etc.[74] The Cu nanowires were obtained through the following reactions

$$CuCl_2 \cdot 2H_2O + 4H_2O \rightarrow Cu(H_2O)_6^{2+} + 2Cl^- \quad (11)$$

$$Fe + 2OH^- + 6H_2O \rightarrow Fe(H_2O)_6^{2+} + 2O^{2-} + H_2 \quad (12)$$

$$H_2 + Cu(H_2O)_6^{2+} \rightarrow Cu\downarrow + 2H^+ + 6H_2O \quad (13)$$

We can see the morphologies of Cu crystals are quite different when we choose different materials, Zn or Fe powder (Fig. 9d,e) and with or without adding 1mL H$_2$O (Fig. 9e,f). We have already mentioned that the acidity (pH$_2$O value) of the hydroxide melts can affect the dissolution of the reactant. However, the intrinsic dissolubility of a material also plays an important role in the crystal growth process. As Zn powder is easier to dissolve than Fe powder in the melts,[75] the Cu crystals prepared from Zn powder have a larger size than those prepared from Fe powder. We have proposed that the addition of a small amount of water can vary the acidity of the hydroxide melts. On the other hand, a small amount of water also can reduce the viscosity of the melts. When the viscosity of the melts is increased by removing the additional water, the product Cu grows into nanowires, due
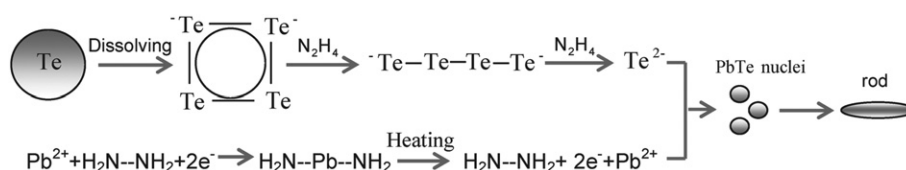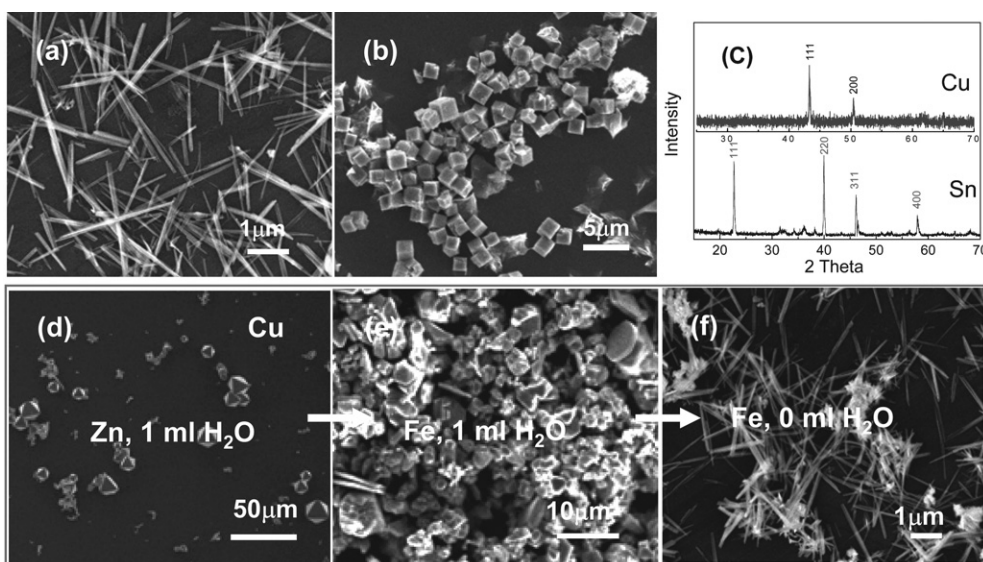

Scheme 1 Illustration of the formation process of PbTe nanorods.[73]
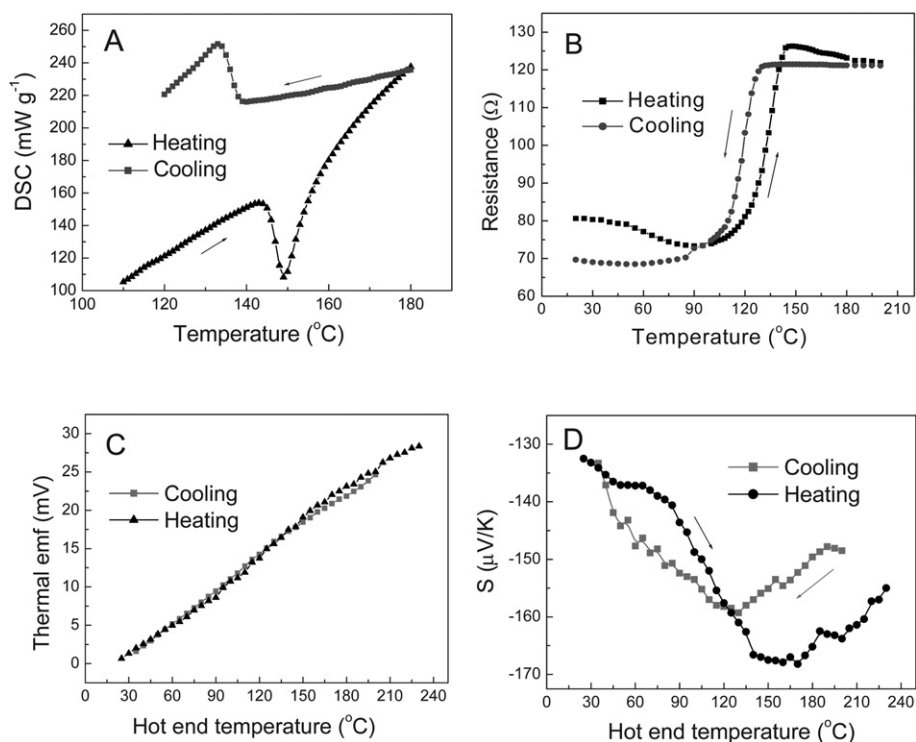
Fig. 8 DSC curves of the Ag$_2$Te nanowires (A). Plots of temperature vs. electrical resistance (B), temperature vs. thermal emf (C) and temperature vs. Seebeck coefficient (D) of the as-prepared silver telluride nanowire film.[50]

Fig. 9 SEM images of Cu nanowires synthesized at 200 °C for 16 h (a), Sn microcubes synthesized at 200 °C for 6 h (b), XRD spectra of the produced Cu and Sn nanocrystals (c), and Cu crystals synthesized from 0.5 mmol CuCl$_2$·2H$_2$O with 0.5 mmol Zn powder and 1 mL H$_2$O (d), with 0.5 mmol Fe powder and 1 mL H$_2$O (e) and with 0.5 mmol Fe powder (f) at 200 °C for 16 h.[74]

to the slower transport of matter. Therefore, here we come to another conclusion that the change of a material can tune the morphology of the crystals using the CHM method.

Fluorides

Fluorides have wide applications in optics, as windows, biological labels, and lenses,[76–78] as well as components of insulators, gate dielectrics, wide-gap insulating overlayers, and buffer layers in semiconductor-on-insulator structures.[79] In addition, fluorides doped with rare-earth ions such as Eu^{3+}, Nd^{3+}, and Ho^{3+} have also been reported to have displayed unique luminescence properties with useful applications in diagnostics, lasing, solid-state light emitters, light amplification, optical telecommunication, and upconversion.[80–82] Hence, it is reasonable to expect that nanoscale fluorides will play an important role in technological
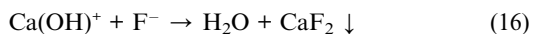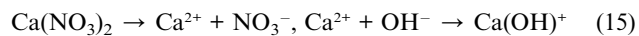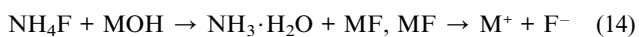
This journal is © The Royal Society of Chemistry 2009

J. Mater. Chem., 2009, **19**, 858–868 | 865
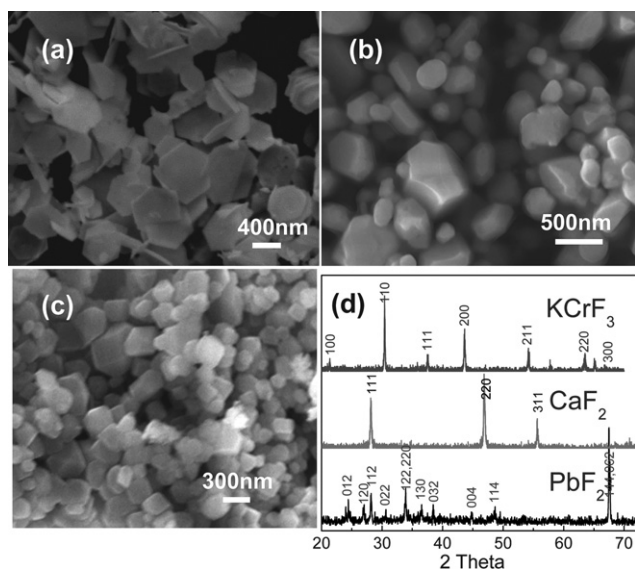
Fig. 10 SEM images of fluoride nanocrystals prepared at 200 °C for 24 h: PbF_2 nanocrystals from materials of NH_4HF_2 and $Pb(NO_3)_2$ (a), CaF_2 nanocrystals from materials of NH_4F and $Ca(NO_3)_2$ (b), and $KCrF_3$ nanocrystals from materials of NH_4F and $Cr(NO_3)_3 \cdot 9H_2O$ (c). XRD spectra of these fluoride nanocrystals (d).[86]

applications including high-density optical storage devices, nanosensors, and color displays.[83–85]

Fluorides have been synthesized by the CHM approach from the materials of metallic salts and NH_4HF_2 or NH_4F or NaF_2 at a temperature of 165–200 °C for 6–24h. Taking the synthesis of CaF_2 nanocrystals as an example, nanocrystals can be obtained from 0.5 mmol $Ca(NO_3)_2$ and 0.5 mmol of NH_4F at 200 °C for 24h (Fig. 10a,d). Other fluorides, PbF_2 and $KCrF_3$ particles, have also been obtained by the CHM approach (Fig. 10b–d).[86]

The formation of CaF_2 follows the reactions (where M = K or Na):

$$NH_4F + MOH \rightarrow NH_3 \cdot H_2O + MF, \; MF \rightarrow M^+ + F^- \quad (14)$$

$$Ca(NO_3)_2 \rightarrow Ca^{2+} + NO_3^-, \; Ca^{2+} + OH^- \rightarrow Ca(OH)^+ \quad (15)$$

$$Ca(OH)^+ + F^- \rightarrow H_2O + CaF_2 \downarrow \quad (16)$$

General schematic diagram

In order to understand the CHM approach better, we present a general schematic illustration showing the CHM preparation procedure applicable for different materials in Fig. 11. Basically, metallic cations of all the target materials are provided by a soluble metallic salt, and anions of them are from different chemicals depending on the composition of the target compound. For complex oxides the anions, oxygen, are from simple oxides. For chalcogenides, the anions are from elemental S, Se, Te powder which are reduced by reducing agents, such as N_2H_4 or $H_2NCH_2CH_2NH_2$. For fluorides, the anions are from some soluble fluorides, such as NH_4HF_2 or NH_4F or NaF_2. Alternatively, metal cations react directly with the medium to produce hydroxides or dehydrate into simple oxides. In addition,
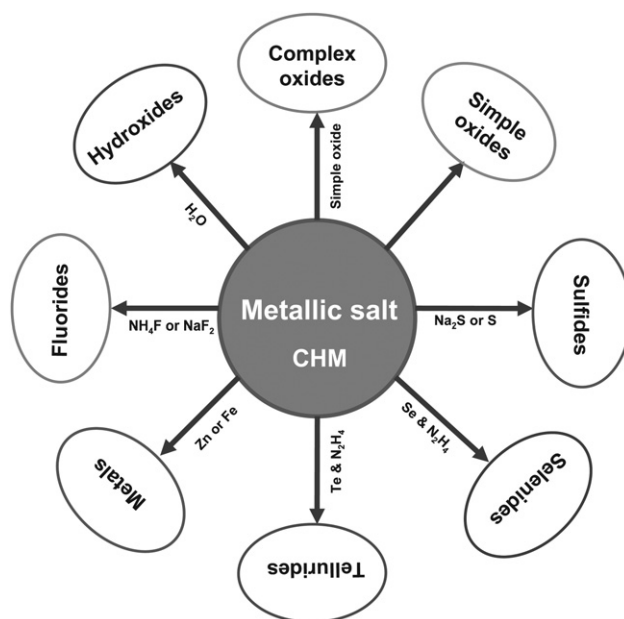
Fig. 11 A general schematic diagram showing the CHM preparation procedure for synthesizing a wide range of nanomaterials.

metal cations can be reduced to elemental metal by H_2 which is reduced from hydroxides by Zn or Fe powder.

4 Summary and perspectives

In this review, we have presented the composite-hydroxide-mediated (CHM) method for preparing nanostructures ranging from complex oxides, hydroxides, simple oxides, sulfides, selenides, tellurides, elemental metal and fluorides. We have demonstrated that the CHM approach is a general methodology for synthesizing nanomaterials (some micromaterials) of a diversity of structures and compositions. Moreover, at the same time, we have concluded that dissolubility of reactants and viscosity of the hydroxide melts are two other important factors that affect the crystal growth by the CHM approach besides the growth time and temperature. Through analysis, we have further proved that the crystal growth experiences the dissolution–crystallization–aggregation–recrystallization process in the composite hydroxide melts. High dissolvability of hydroxide melt is beneficial to the dissolution of the reactants, and reaction among the reactants, while high viscosity prevents crystals from growing large. The dissolubility of reactants can be adjusted by varying the acidity (pH_2O value) of the melts and by choosing different reaction materials according to their intrinsically dissoluble potentials in the melts. The viscosity can be manipulated by altering the temperature and by changing the acidity of the melts. A suitable dissolubility of reactants and viscosity of the melts can help us obtain well-defined morphology of the desired crystals.

The CHM approach has unique advantages. (1) It is a simple, one-step and slow-reaction synthesis approach, making it possible to control growth kinetics for the purpose of tuning the size and morphology of the synthesized nanostructures. (2) The synthesis is carried out at a low growth temperature of ∼200 °C in ambient atmosphere, and it needs no expensive or

sophisticated equipment; thus, the technique is potentially easy to be adopted and transferred for technological applications. (3) The reaction materials are not expensive and the entire synthesis process is cost effective. The yield is high and it can be readily expandable for large-scale production. (4) Most of the as-produced nanostructures are high quality single crystals, which are fit for the requirements of many applications. (5) There is no capping reagent on the surfaces of the as-synthesized nanostructures, thus, the clean surfaces can be readily functionalized for various purposes. (6) The synthesis process is nontoxic and does not produce any hazardous waste. The used hydroxide solution could be reused after a simple treatment. For example, there are extra Cl^- ions (from equation 6 and 7) in the residual solution in the process of synthesizing Cu_2O. We could remove Cl^- from the solution through electrochemical methods. After evaporating the water in the solution, pure hydroxides are obtained. (7) The method can be expanded to many materials categories and, certainly, it provides a general, simple, convenient and innovative strategy for synthesis of nanostructures with important scientific and technological applications.

We have long-standing goals of creating well-defined nanoscale building blocks with tailorable properties. We have been interested in relatively simple synthesis methods whose ideal attributes include stability as well as good control of size, shape, morphology, and chemical composition in the final product. It is evident that the cost-effective techniques we have described herein are a step in the right direction towards developing processes that allow for quality and quantity of the synthesized products with minimal impact on the environment. Of course, the method requires constant optimization as well as real-time, in-process monitoring. In our future work, electrochemical monitoring will be carried out to probe the kinetics and mechanism of the CHM route. We will also consider combining a small amount of salt with the composite hydroxides to control the crystal growth dynamics. On the other hand, the salt (such as NaCl) in the residual solution could be an effective composition of the composite medium and recycle utilization of the waste could be realized.

References

1 C. F. Pan, H. Wu, C. Wang, B. Wang, L. Zhang, Z. D. Cheng, P. Hu, W. Pan, Z. Y. Zhou, X. Yang and J. Zhu, *Adv. Mater.*, 2008, **20**, 1644.
2 U. Bach, D. Lupo, P. Comte, J. E. Moser, F. Weissörtel, J. Salbeck, H. Spreitzer and M. Graätzel, *Nature*, 1998, **395**, 583.
3 B. Tian, X. Zheng, T. J. Kempa, Y. Fang, N. Yu, G. Yu, J. Huang and C. M. Lieber, *Nature*, 2007, **449**, 885.
4 Y. G. Guo, J. S. Hu and L. J. Wan, *Adv. Mater.*, 2008, **20**, 2878.
5 Z. P. Shao and S. M. Haile, *Naure*, 2004, **431**, 170.
6 Z. H. Bao, M. R. Weatherspoon, S. Shian, Y. Cai, P. D. Graham, S. M. Allan, G. Ahmad, M. B. Dickerson, B. C. Church, Z. Kang, C. J. Summers, H. W. Abernathy,III, M. Liu and K. H. Sandhage, *Nature*, 2007, **446**, 172.
7 A. Serpengüzel, A. Kurt, I. Inanç, J. E. Cary and E. Mazur, *J. Nanophotonics*, 2008, **2**, 021770.
8 J. Zhou, Y. D. Gu, P. Fei, W. J. Mai, Y. F. Gao, R. S. Yang, G. Bao and Z. L. Wang, *Nano Letters*, 2008, **8**, 3035.
9 L. Shang and S. J. Dong, *J. Mater. Chem.*, 2008, **18**, 4636.
10 F. Patolsky, G. Zheng and C. M. Lieber, *Anal. Chem.*, 2006, **78**, 4260.
11 Y. Li, F. Qian, J. Xiang and C. M. Lieber, *Materials Today*, 2006, **9**, 18.
12 Z. L. Wang, *Adv. Func Mater.*, 2008, **18**, 1.
13 M. H. Huang, S. Mao, H. Feick, H. Yan, Y. Y. Wu, H. Kind, E. Weber, R. Russo and P. Yang, *Science*, 2001, **292**, 1897.
14 T. Voss, G. T. Svacha, E. Mazur, S. Muüller, C. Ronning, D. Konjhodzic and F. Marlowet, *Nano Lett.*, 2007, **7**, 675.
15 P. G. Collins, A. Zettl, H. Bando, A. Thess and R. E. Smalley, *Science*, 1997, **278**, 100.
16 J. Xiang, W. Lu, Y. Hu, Y. Wu, H. Yan and C. M. Lieber, *Nature*, 2006, **441**, 489.
17 C. Falconi, A. D'Amico and Z. L. Wang, *Sensors and Actuators B*, 2007, **127**, 54.
18 J. Gamby, J. P. Abid, B. Tribollet and H. H. Girault, *Small*, 2008, **4**, 802.
19 W. C. W. Chan and S. M. Nie, *Science*, 1998, **281**, 2016.
20 A. M. Smith, H. W. Duan, A. M. Mohs and S. M. Nie, *Adv. Drug Delivery Rev.*, 2008, **60**, 1226.
21 Y. B. Mao, T. J. Park, F. Zhang, H. J. Zhou and S. S. Wong, *Small*, 2007, **3**, 1122.
22 J. P. Xie, J. Y. Lee, D. I. C. Wang and Y. P. Ting, *ACS nano*, 2007, **1**, 429.
23 P. Raveendran, J. Fu and S. L. Wallen, *Green Chem.*, 2006, **8**, 34.
24 L. C. McKenzie and J. E. Hutchison, *Chem. Today*, 2004, **22**, 30.
25 Z. W. Pan, Z. R. Dai and Z. L. Wang, *Science*, 2001, **291**, 1947.
26 Y. Wu, J. Xiang, C. Yang, W. Lu and C. M. Lieber, *Nature*, 2004, **430**, 61.
27 J. E. Lee, S. M. Oh and D. W. Park, *Thin Solid Films*, 2004, **457**, 230.
28 Y. J. Tian, Y. P. Jia, Y. J. Bao and Y. F. Chen, *Diam. Rel. Mater.*, 2007, **16**, 302.
29 D. Kuscer, J. Holc and M. Kosec, *J. Am. Ceramic Soc.*, 2007, **90**, 29.
30 T. P. Yadav, N. K. Mukhopadhyay and R. S. Tiwari, *J. Nanosci, Nanotech.*, 2007, **7**, 575.
31 M. Cernea, O. Monnereau, P. Llewellyn, L. Tortet and C. Galassi, *J. Eur. Ceramic Soc.*, 2006, **26**, 3241.
32 A. Hartridge and A. K. Bhattacharya, *J. Phys. Chem. Solids*, 2002, **63**, 441.
33 X. Zhang and K. Y. Chan, *Chem. Mater.*, 2003, **15**, 451.
34 A. S. Deshpande, N. Pinna, P. Beato, M. Antonietti and M. Niederberger, *Chem. Mater.*, 2004, **16**, 2599.
35 B. B. Lakshmi, C. J. Patrissi and C. R. Martin, *Chem. Mater.*, 1997, **9**, 2544.
36 H. Song, R. M. Rioux, J. D. Hoefelmeyer, R. Komor, K. Niesz, M. Grass, P. Yang and G. A. Somorjai, *J. Am. Chem. Soc.*, 2006, **128**, 3027.
37 H. G. Yang, C. H. Sun, S. Z. Qiao, J. Zou, G. Liu, S. C. Smith, H. M. Cheng and G. Q. Lu, *Nature*, 2008, **453**, 638.
38 A. W. Xu, Y. P. Fang, L. P. You and H. Q. Liu, *J. Am. Chem. Soc.*, 2003, **125**, 1494.
39 L. E. Greene, B. D. Yuhas, M. Law and P. Yang, *Inorg. Chem.*, 2006, **45**, 7535.
40 K. B. Zhou, X. Wang, X. M. Sun, Q. Peng and Y. D. Li, *J. Catalysis*, 2005, **229**, 206.
41 X. Wang, J. Zhuang, Q. Peng and Y. D. Li, *Nature*, 2005, **437**, 121.
42 J. L. Luce and A. M. Stacy, *Chem. Mater.*, 1997, **9**, 1508.
43 K. E. Stitzer, M. D. Smith and H. C. Z. Loye, *Solid State Sci.*, 2002, **4**, 311.
44 S. J. Mugavero III, M. D. Smith and H. C. Z. Loye, *Inorg. Chem.*, 2007, **46**, 3116.
45 S. J. Mugavero III, M. D. Smith and H. C. Z. Loye, *J. Solid State Chem.*, 2006, **179**, 3586.
46 C. M. S. Shivakumara, A. S. Hegde, A. M. A. Prakash, G. N. Khadar and N. P. L. Subbanna, *Solid State Sci.*, 2003, **5**, 351.
47 H. Liu, C. G. Hu and Z. L. Wang, *Nano Lett.*, 2006, **6**, 1535.
48 C. G. Hu, H. Liu, C. S. Lao, L. Y. Zhang, D. Davidovic and Z. L. Wang, *J. Phys. Chem. B*, 2006, **110**, 14050.

This journal is © The Royal Society of Chemistry 2009

J. Mater. Chem., 2009, **19**, 858–868 | 867

49 C. G. Hu, H. Liu, W. T. Dong, Y. Y. Zhang, G. Bao, C. S. Lao and Z. L. Wang, *Adv. Mater.*, 2007, **19**, 470.
50 F. Y. Li, C. G. Hu, Y. F. Xiong, B. Y. Wan, W. Yan and M. C. Zhang, *J. Phys. Chem. C*, 2008, **112**, 16130.
51 N. Wang, C. G. Hu, C. H. Xia, B. Feng, Z. W. Zhang, Y. Xi and Y. F. Xiong, *Appl. Phys. Lett.*, 2007, **90**, 163111.
52 Z. W. Zhang, C. G. Hu, Y. F. Xiong, R. S. Yang and Z. L. Wang, *Nanotechnology*, 2007, **18**, 465504.
53 M. C. Zhang, C. G. Hu, H. Liu, Y. Y. Xiong and Z. W. Zhang, *Sensors and Actuators B*, DOI: 10.1016/j.snb.2008.09.021.
54 J. Miao, C. G. Hu, Y. F. Xiong, X. Y. Han and Y. Xi, *Acta Phys.-Chim. Sin.*, 2007, **23**, 1599.
55 H. L. Chen and C. P. Grey, *Adv. Mater.*, 2008, **20**, 2206.
56 K. C. Zhang, *Basics in Modern Crystallology*, vol. 2, Science Press, Bejing, 1987, pp. 76–133.
57 T. Sugimoto, *Adv. Colloid Interface Sci.*, 1987, **28**, 65.
58 J. Goret, *Bull. Soc. Chim.*, 1964, (5), 1074.
59 R. G. Doisneau and B. Tremillon, *J. Chim. Phys.*, 1974, **71**, 1445.
60 H. W. Otto and R. P. Seward, *J. Chem. Eng. Data*, 1964, **9**, 507.
61 C. G. Hu, J. Mia, H. Liu, Z. Q. Liu and Y. F. Xiong, *J. Nanosci. Nanotech.*, 2008, **8**, DOI: 10.1166/jnn.2008.1099.
62 Z. M. Liao, K. J. Liu, J. M. Zhang, J. Xu and D. P. Yu, *Phys. Lett. A*, 2007, **367**, 207.
63 E. J. Cussen and P. D. Battle, *Chem. Mater*, 2000, **12**, 831.
64 Y. M. Wang, G. J. Du, H. Liu, D. Liu, S. B. Qin, N. Wang, C. G. Hu, X. T. Tao, J. Jiao, J. Y. Wang and Z. L. Wang, *Adv. Funct. Mater.*, 2008, **18**, 1131.
65 C. Burda, X. B. Chen, R. Narayanan and M. A. El-Sayed, *Chem. Rev.*, 2005, **105**, 1025.
66 Y. Xi, C. G. Hu, R. S. Yang, B. Feng, X. S. He and X. Wang, submitted.
67 C. G. Hu, Z. W. Zhang, H. Liu, P. X. Gao and Z. L. Wang, *Nanotechnology*, 2006, **17**, 5983.
68 C. Dauby, J. Glibert and P. Clase, *Electrochim. Acta*, 1979, **24**, 35.
69 J. Mukesh, (ed.) *II–VI semiconductor Compounds*. World Scientific, Singapore, 1993.
70 C. G. Hu and Y. Xi, Patentpending, Open No. CN101112974, Jun. 21, 2007.
71 C. G. Hu, Y. Xi, Z. L. Wang, W. Yan, B. Y. Wan, M. C. Zhang and F. Y. Li, Patent pending, Open No. CN101219779, Jan. 14, 2008.
72 W. S. Sheldrick and M. Wachhold, *Angew. Chem. Int. Ed. Engl.*, 1997, **36**, 207.
73 B. Y. Wan, C. G. Hu, H. Liu, Y. F. Xiong, F. Y. Li, Y. Xi and X. S. He, submitted.
74 Y. Xi, C. G. Hu and Z. L. Wang, Patent pending, Open No. CN101279374, Jan. 14, 2008.
75 J. A. Dean, *Lange's Handbook of Chemistry*, 15th ed.; McGraw-Hill: New York, 1999.
76 C. M. Bender, J. M. Burlitch, D. Barber and C. Pollock, *Chem. Mater.*, 2000, **12**, 1969.
77 H. Lian, J. Liu, Z. Ye and C. Shi, *Chem. Phys. Lett.*, 2004, **386**, 291.
78 R. Hua, C. Zang, C. Shao, D. Xie and C. Shi, *Nanotechnology*, 2003, **14**, 588.
79 R. Singh, S. Sinha, P. Chou, N. J. Hsu and F. Radpour, *J. Appl. Phys.*, 1989, **66**, 6179.
80 L. F. Johnson and H. J. Guggenheim, *Appl. Phys. Lett.*, 1971, **19**, 44.
81 X. X. Zhang, P. Hong, M. Bass and B. H. T. Chai, *Phys. Rev. B*, 1995, **51**, 9298.
82 P. Xie and S. C. Rand, *Opt. Lett.*, 1992, **17**, 1198.
83 M. Cao, C. Hu and E. Wang, *J. Am. Chem. Soc.*, 2003, **125**, 11196.
84 M. Cao, Y. Wang, Y. Qi, C. Guo and C. Hu, *J. Solid State Chem.*, 2004, **177**, 2205.
85 G. De, W. Qin, J. Zhang, D. Zhao and J. Zhang, *Chem. Lett.*, 2005, **34**, 914.
86 M. C. Zhang, C. G. Hu, Y. F. Xiong, Y. Xi, F. Y. Li and W. Yan, *J. Funct. Mater.*, in press.